



## 2-D numerical study of ferrofluid droplet formation from microfluidic T-junction using VOSET method

Shuai Zhang, Kong Ling, Na Sun, Siyuan Yang, Xiangmiao Hao, Xiaowei Sui & Wen-Quan Tao

To cite this article: Shuai Zhang, Kong Ling, Na Sun, Siyuan Yang, Xiangmiao Hao, Xiaowei Sui & Wen-Quan Tao (2021) 2-D numerical study of ferrofluid droplet formation from microfluidic T-junction using VOSET method, Numerical Heat Transfer, Part A: Applications, 79:9, 611-630, DOI: 10.1080/10407782.2021.1872283

To link to this article: <https://doi.org/10.1080/10407782.2021.1872283>



Published online: 01 Feb 2021.



Submit your article to this journal [↗](#)



Article views: 107



View related articles [↗](#)



View Crossmark data [↗](#)



Citing articles: 1 View citing articles [↗](#)



## 2-D numerical study of ferrofluid droplet formation from microfluidic T-junction using VOSET method

Shuai Zhang<sup>a,b</sup>, Kong Ling<sup>a,b</sup>, Na Sun<sup>c</sup>, Siyuan Yang<sup>b</sup>, Xiangmiao Hao<sup>b</sup>, Xiaowei Sui<sup>d</sup>, and Wen-Quan Tao<sup>a</sup>

<sup>a</sup>Key Laboratory of Thermo-Fluid Science & Engineering of MOE, Xi'an Jiaotong University, Shaanxi, P.R. China; <sup>b</sup>Xi'an ShuFeng Technological Information, Ltd, Shaanxi, P.R. China; <sup>c</sup>College of Automation, Huaiyin Institute of Technology, Jiangsu, P.R. China; <sup>d</sup>Department of Creative Design, National Institute Corporation of Additive Manufacturing Xi'an, Shaanxi, P.R. China

### ABSTRACT

This article conducts a two-dimensional numerical model to simulate the ferrofluid droplet formation from microfluidic T-junction under inhomogeneous magnetic fields with diverse strengths. This external magnetic field is produced by two electric straight wires in a finite computational domain. A coupled volume-of-fluid and level-set interface tracking method (VOSET) is adopted to capture the evolution of two-phase interface. Meanwhile, a two-region computational domain method is designed for situations that the droplets are in close contact with the solid boundaries for the fluid flow. All 2-D numerical simulations are implemented by a self-developed CFD code, named as MHT (Multi-concept Heat Transfer). The numerical results show a significant inhibition effect in droplet formation at the presence of external magnetic field. With the increase of the current intensity, the magnetic force of the ferrofluid droplet increases and decreases periodically, especially when the electric current intensity is less than 60 A. The increasing current intensity enlarges the departure diameter and prolongs the departure period of ferrofluid droplet, especially when the current intensity in the range 12 A~54 A. In the cases of electric current within [12 A, 54 A], the departure diameter grows monotonically and nearly in a quadratic manner with the increase of the current intensity. However, when the current intensity exceeds 60 A, the departure characteristic of ferrofluid will be changed due to ferrofluid droplet absorbed on the upper wall of the main channel.

### ARTICLE HISTORY

Received 7 November 2020  
Accepted 6 December 2020

## 1. Introduction

Ferrofluid is an artificial material having both properties of magnetic material and fluid. Due to its unique features, it is widely applied in sealing, sensing, vibration damping, optics, biomedicine, and other fields[1].

With the continuous development of micro-fabrication technology, ferrofluids have been applied to small scale devices, such as nanoscale self-assembly [2], magnetic trapping of bacteria [3], micropumps [4], drug delivery [5] and magnetic cell separation [6]. Because ferrofluid droplets can be used as carriers for transporting samples or as reaction platforms for lab-on-a-chip (LoC) applications, accurate positioning of ferrofluid droplets is very important. In recent years,

**CONTACT** Wen-Quan Tao  [wqtao@mail.xjtu.edu.cn](mailto:wqtao@mail.xjtu.edu.cn)  Key Laboratory of Thermo-Fluid Science & Engineering of Ministry of Education (MOE), School of Energy and Power Engineering Xi'an Jiaotong University, 28 Xianning west Road, Xi'an, Shaanxi 710049 P.R. China.

most studies of ferrofluid are focused on the shape of droplets or on observing the droplets formation processes through experiments. For instance, Fabian et al. [7] experimentally explored the influence of parallel and perpendicular homogenous magnetic field on the ferrofluid droplet formation in dripping regime. Zhang et al. [8] experimentally investigated the ferrofluid droplet formation in a microfluidic T-junction, and a non-uniform magnetic field was constructed by a permanent magnet placed at one side of the junction. Their results found an effect of the magnetic field in prolonging the generation cycle. Sun et al. [9] used a high-speed digital camera to observe the dynamics for droplet breakup with tunnels and formation of satellite droplets in a symmetric microfluidic T-junction. Favakeh et al. [10] reported ferrofluid droplet formation in the presence of alternating magnetic field. All these experimental observations on the ferrofluid droplets manipulation suggest that the dynamic behavior of ferrofluid droplets can be controlled by the integrating action of both the magnetic field and flow field. However, a deep insight into the flow behavior and the mechanism of ferrofluid droplets placed in magnetic fields is still lacking.

With the advance of robust numerical algorithms and the rapid development of computer hardware, numerical simulation has been becoming an ever-increasing powerful tool to achieve a deeper understanding of basic mechanism and characteristics of complicated physical processes, such as the action of ferrofluid droplets under an external magnetic field. Relying on numerical simulation tools, researchers can further reveal the coupling physical mechanism of magnetic field and flow field. However, due to the complexity of two-phase flow problem with an external magnetic field, the corresponding numerical approaches are still in development. Followings are a brief review in this regard. Lavrova et al. [11] proposed a numerical solution strategy based on finite element method (FEM) for calculating equilibrium free surfaces of ferrofluid under a magnetic field and determined the shapes of a ferrofluid droplet in a uniform magnetic field. Several years later, Korlie et al. [12] developed a volume-of-fluid (VOF) method to study the dynamic behavior of ferrofluid droplets exposed in a uniform magnetic field. Afkhami et al. [13] investigated the deformation of a biocompatible ferromagnetic droplets suspended in viscous media in presence of uniform magnetic field, and their results indicated the droplet extending along the direction of the magnetic field. In the same year, Ki [14] addressed the numerical simulation for two-phase incompressible flows in the presence of magnetic fields by using the level-set method. Later, Liu et al. [15] performed numerical studies on the process of ferrofluid droplet formation subjected to a uniform magnetic field paralleling with the flow direction and compared with the experimental results. The results show that under the effect of the external magnetic field, longer formation time and larger formation size of droplets can be observed due to the pulling effect on the tip of droplets. Based on this, they also applied a particle level-set method on the simulation of this problem and obtained similar results [16]. Shi et al. [17] performed a 2-D numerical simulation on ferrofluid droplet falling in a nonmagnetic fluid subjected to a uniform magnetic force. In the simulations, the method of VOSET [18] was used to capture the evolution of interface. The effects of some parameters such as the magnetic Bond number, susceptibility, Weber number, Reynolds number, and magnetic field direction on the motion and deformation of droplet were investigated systematically. The results obtained by their simulations indicated that an increase in magnetic Bond number or susceptibility results in a greater degree of the droplet deformation. In the next year, Ghaffari et al. [19] simulated the deformation of ferrofluid droplet under a uniform magnetic field and investigated some parameters influencing the droplet shape at equilibrium including the magnetic field intensity, droplet size, and surface tension. In their simulations, the CFD package OpenFOAM with CLSVOF method [20] was applied to capture the interface. From the data collected in their simulations, a correlation was proposed for the prediction of the aspect ratio at equilibrium. Sen et al. [21] employed VOF to track the interface and numerically simulated ferrofluid droplet generation in a T-junction considering a magnetic field generated by two magnetic dipoles. In their study, it was assumed that the ferrofluid does not change the magnetic field. Habera and Hron [22] developed a numerical approach based on FEM

to solve the Maxwell's equations for ferrofluid free surface flows. In their research, equilibrium droplet shapes were numerically studied and compared with the experimental results. Varma et al. [23] conducted LoC experimental and numerical investigations on the manipulation of ferrofluid droplets in a uniform magnetic field. The result suggests that droplet size, shape, inter-droplet space and velocity can be controlled by adjusting the magnetic permeability, the viscosity, and the flow rate of carrier medium. Based on this, Ray et al. [24] investigated the manipulation of ferrofluid droplets in a capillary microfluidic platform by a combination of uniform and non-uniform magnetic fields.

Numerical simulation studies are further developed in recent two years. Aboutalebi et al. [25] performed a numerical simulation on the splitting process of ferrofluid droplet in a T-junction under a magnetic field. In the presence of an asymmetric magnetic field, they observed the unequal separation sizes of the child droplets at the junction. Hassan et al. [26] numerically simulated the deformation and orientation of a ferrofluid droplet in a simple shear flow under a uniform magnetic field. They applied conservative level set method for droplet interface tracking. Ghaderi et al. [27] proposed a robust 2-D hybrid lattice-Boltzmann/FEM coupled magnetic field equations and did a series of numerical simulations on the behavior of ferrofluid droplet falling in nonmagnetic fluid under a uniform field. A mathematical model for a ferrofluid droplet in a simple shear flow in the presence of a uniform magnetic field is elaborated by Paolo et al. [28]. Their results revealed that the droplet deformation is affected by the applied magnetic field intensity and varies in time following a harmonic decaying law. Ling et al. [29] carried out a numerical investigation on the motion of a ferrofluid droplet in a non-uniform magnetic field produced by an electric wire loop. Their results show that the net magnetic force imposed on the droplet can overcome the gravity and prevent it from dropping.

As can be seen, although a number of numerical studies have been conducted on the behaviors of ferrofluid droplets under uniform/nonuniform magnetic field, research on the formation of ferrofluid droplets in a microfluidic T-junction under nonuniform magnetic field is very limited. Additionally, when a ferrofluid droplet is placed in a magnetic field, it will distort the magnetic lines around it due to its greater magnetic permeability than non-magnetic materials. In the existing studies, the magnetic field was solved in a computational domain designed for fluid flow. It requires the computational domain be large enough such that its borders are sufficiently far from the interface between the ferrofluid and non-magnetic fluid phases. However, in many applications, ferrofluid droplets are controlled in narrow space, such as ferrofluid pump [4] and valve used in microchips [30]. In those situations, the droplets are in close contact with the solid boundaries for the fluid flow. To resolve this issue, a new scheme of computational domain should be proposed.

In this article an in-house Multi-concept Heat Transfer (MHT) code developed by the authors' group is applied to simulate the motion and deformation of ferrofluid droplets in a microfluidic T-junction under an inhomogeneous magnetic field. A two-region computational domain is adopted, in which the magnetic field is solved in an extended domain. To test this in-house code, the formation of a single ferrofluid droplet under a uniform magnetic field is first simulated. Numerical simulations using MHT code are conducted for the motion and deformation of ferrofluid droplets in a non-uniform magnetic field. The numerical simulation results are discussed at various parameters considering effects of magnetic force. The obtained results can provide valuable references for accurately controlling the size and frequency of ferrofluid droplets.

The rest of this article is structured as follows. [Section 2](#) presents the ferrofluid free surface flow from the physical point of view and gives its governing equations; and [Section 3](#) describes the numerical methods for solving those equations. [Section 4](#) presents and discusses some numerical simulations, including validations of the adopted in-house code. Finally, some conclusions were drawn in [Section 5](#).

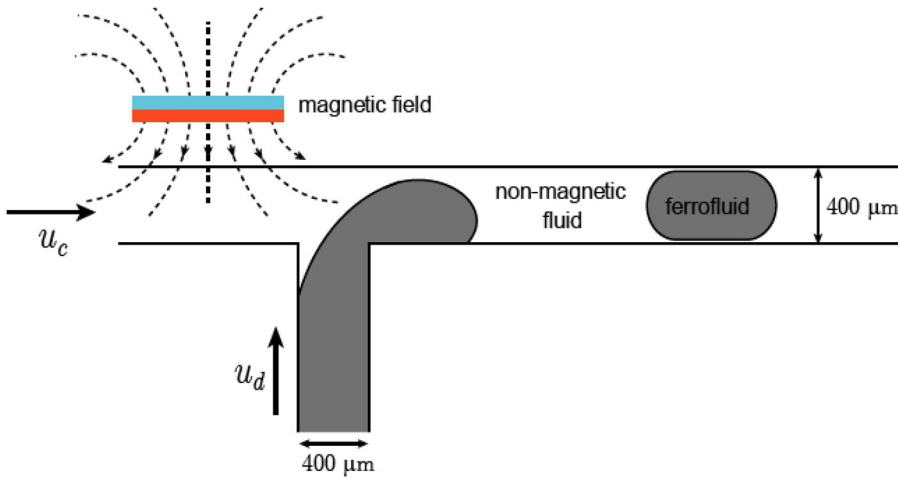


Figure 1. Schematic of microfluidic T-junction droplet generator.

## 2. Problem description

Figure 1 provides the schematic of a two-dimensional microfluidic T-junction droplet generator considered in the present study. The ferrofluid (dispersed phase) and a non-magnetic fluid (continuous phase) are injected from the main channel and the branch one, respectively. Under the influence of the continuous phase, the ferrofluid flows into the main channel in droplets with a certain size, which varies with the flow rates of the two phases. Meanwhile, a non-uniform magnetic field is applied around the channel junction, which applies a volumetric force on the ferrofluid. It will therefore influence the splitting process and vary the size of the generated droplets. The main and the branch channels are both  $400\ \mu\text{m}$  in width. The properties of the water-based ferrofluid, and the non-magnetic fluid reported by Zhang et al. [8] are adopted here. Densities of the non-magnetic fluid and the ferrofluid are  $\rho_c = 872.5\ \text{kg/m}^3$  and  $\rho_d = 1100\ \text{kg/m}^3$ , respectively; their viscosities are  $\eta_c = 0.026\ \text{Pa}\cdot\text{s}$  and  $\eta_d = 0.002\ \text{Pa}\cdot\text{s}$ , respectively. The susceptibility of the ferrofluid is  $\chi = 2.88$  at the particle volume concentration of 2%, and the surface tension coefficient between the two phases is  $\sigma = 0.0015\ \text{N/m}$ . All physical properties of the two phases are listed in Table 1.

It is worth noting that the non-uniform magnetic field in this study (as schematically shown in Figure 2) is generated by two electrified straight wires (see Eq. (1)) instead of the permanent magnet reported in [8]. This unique design is based on the fact that the magnetic field generated by the energized line can be easily altered by changing its current value. Under this condition, we can modulate the magnetic field strength by changing the magnitude of the electric current. This change of magnetic field will lead to the variation of the joint influence of the magnetic force, gravity, and surface tension, which will affect the splitting process and change the size of the generated ferrofluid droplets.

$$\mathbf{H}(x, y) = \frac{\mathbf{I} \times (\mathbf{P} - \mathbf{P}_1)}{2\pi|\mathbf{P} - \mathbf{P}_1|^2} - \frac{\mathbf{I} \times (\mathbf{P} - \mathbf{P}_2)}{2\pi|\mathbf{P} - \mathbf{P}_2|^2} \quad (1)$$

where the locations of  $\mathbf{P}_1$  and  $\mathbf{P}_2$  are  $(0.000\ \text{m}, 0.002\ \text{m})$  and  $(0.001\ \text{m}, 0.002\ \text{m})$ , respectively.

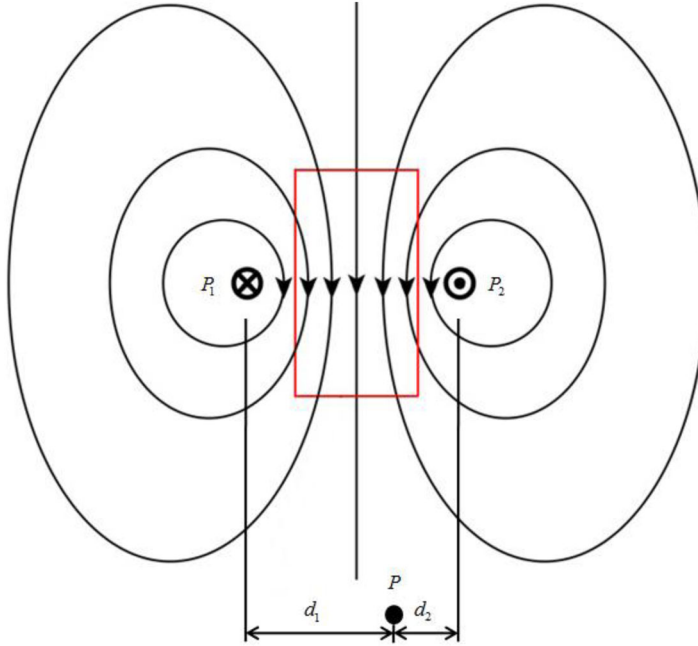
### 2.1. Physical assumptions

The flow of ferrofluid droplets in magnetic field can be treated as a problem of incompressible free surface flow with interaction between a dispersed phase and a continuous one. Ferrofluid

**Table 1.** Physical properties of the continuum and the dispersed phases ([8]).

Phase	Density (kg/m <sup>3</sup> )	Viscosity (N · s/m)	Magnetic permeability	Surface tension (N/m)
Continuum	1100.0	0.002	$\mu_0^*$	–
Dispersed	872.5	0.026	$2.88\mu_0$	0.0015

\* $\mu_0$  is the vacuum permeability and  $\mu_0 = 4\pi \times 10^{-7} \text{N/A}^2$ .


**Figure 2.** Magnetic field generated by two electrified straight wires.

free surface flow in magnetic field is associated with multiple physical processes. Their governing equations are as follows.

### 2.1.1. Governing equation for fluid flow

The fluid flow can be considered as incompressible two-phase flow with moving interfaces. Using the one-fluid formulation, the fluid flow can be described by continuity and momentum equations,

$$\nabla \cdot \mathbf{u} = 0 \quad (2)$$

$$\frac{\partial(\rho\mathbf{u})}{\partial t} + \nabla \cdot (\rho\mathbf{u} \otimes \mathbf{u}) = -\nabla p + \nabla \cdot (\eta\nabla\mathbf{u} + \eta\nabla\mathbf{u}^T) + \rho\mathbf{g} + \mathbf{F}_\sigma + \mathbf{F}_H \quad (3)$$

where the gravity acceleration  $\mathbf{g}$  is specified as  $9.8 \text{ m/s}^2$ ;  $\mathbf{F}_\sigma$  and  $\mathbf{F}_H$  denote the surface tension and the magnetic force, respectively.  $\mathbf{F}_\sigma$  and  $\mathbf{F}_H$  can be calculated by:

$$\mathbf{F}_\sigma = \sigma\kappa\delta(\phi)\mathbf{n} \quad (4)$$

$$\mathbf{F}_H = \nabla \cdot \boldsymbol{\tau}_m$$

$$\boldsymbol{\tau}_m = \left( \mu\mathbf{H}\mathbf{H} - \frac{1}{2}\mu H^2\mathbf{I} \right) \quad (5)$$

### 2.1.2. Governing equation for magnetic field

The magnetic field can be described by the Maxwell's equations for a nonconducting ferrofluid.

$$\nabla \cdot \mathbf{B} = 0 \quad (6)$$

$$\nabla \times \mathbf{H} = 0 \quad (7)$$

$$\mathbf{B} = \mu_0(\mathbf{H} + \mathbf{M}) \quad (8)$$

where  $\mathbf{H}$ ,  $\mathbf{B}$ , and  $\mathbf{M}$  are the magnetic field strength, the magnetic flux density and the magnetization of the ferrofluid, respectively.

In the non-magnetic phase (continuous phase), the magnetization vanishes. According to the linear magnetization assumption for the ferrofluid, the magnetization  $\mathbf{M}$  and magnetic field strength  $\mathbf{H}$  satisfy the relationship  $\mathbf{M} = \chi\mathbf{H}$ . Therefore, magnetic induction  $\mathbf{B}$  can be determined by:

$$\mathbf{B} = \mu\mathbf{H} \quad (9)$$

where  $\mu = (1 + \chi)\mu_0$ . Note,  $\mu$  takes different values in the two phases.

Usually, the ferrofluid phase can be treated as a non-conducting, linear magnetization material. Then, the magnetic field strength  $\mathbf{H}$  can be written as:

$$\mathbf{H} = -\nabla\psi \quad (10)$$

where  $\psi$  represents a magnetic scalar potential.

Combining Eqs. (6), (9) and (10), the governing equation for the magnetic field can be expressed as:

$$\begin{aligned} \nabla \cdot (\mu\nabla\psi) &= 0 \\ \mu &= \mu_0(1 + \chi) \end{aligned} \quad (11)$$

## 3. Numerical methods

The numerical methods presented in this section are implemented by an in-house CFD code, named as MHT, designed for solving multi-region heat transfer and fluid flow. Compared with Fluent and other CFD commercial software, MHT has many advantages such as flexible grid interface, multi-region coupling function, extensible module, and convenient for secondary development. Based on MHT framework, a two-region approach for magnetic field is adopted. Then, the formation of ferrofluid in non-uniform magnetic field is simulated.

### 3.1. Interface tracking method

The volume fraction of the ferrofluid  $f$  satisfies following equation,

$$\frac{\partial f}{\partial t} + \mathbf{u} \cdot \nabla f = 0 \quad (12)$$

Youngs' PLIC algorithm [31] is implemented in interface reconstruction. The jumps of the surface tension and magnetic forces near the interface are handled by a smoothed Heaviside function in the whole computational domain. The smoothed Heaviside function and its derivative, namely smoothed delta function, are given below:

$$H(\phi) = \begin{cases} 0 & \phi < -\varepsilon \\ \frac{1}{2} \left( 1 + \frac{\phi}{\varepsilon} + \frac{1}{\pi} \sin \frac{\pi\phi}{\varepsilon} \right) & -\varepsilon < \phi < \varepsilon \\ 1 & \phi > \varepsilon \end{cases} \quad (13)$$

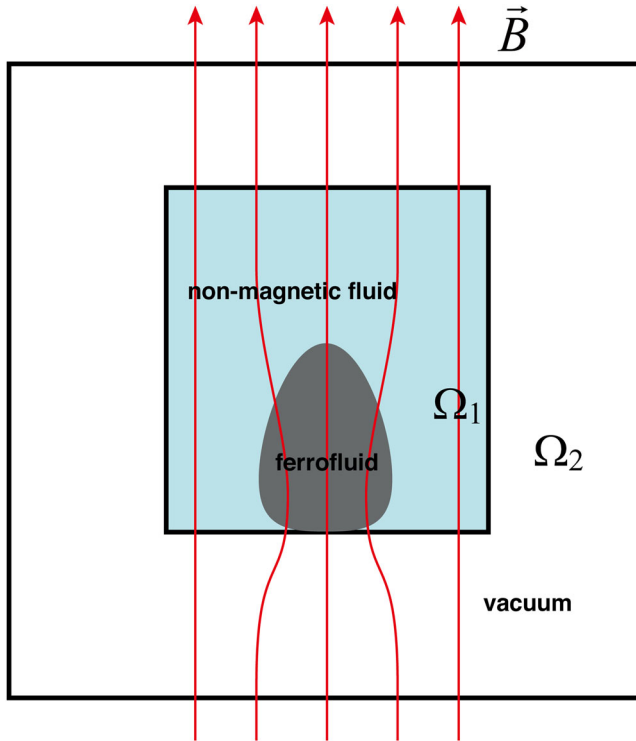


**Figure 3.** Two-region method for ferrofluid free surface flow.

$$\delta(\phi) \begin{cases} 0 & |\phi| > \varepsilon \\ \frac{1}{2\varepsilon} \left( 1 + \cos \frac{\pi\phi}{\varepsilon} \right) & |\phi| \leq \varepsilon \end{cases} \quad (14)$$

where  $\varepsilon$  is an adjustable parameter of size, often taken 1.5 times (or more than) of the mesh size;  $\phi$  represents a Level-Set function and it is generated by the reconstructed interface geometry in VOSET, in order to calculate the interface normal and curvature more accurately.

### 3.2. Two-region approach for the magnetic field

As indicated above, the magnetic field is usually solved in the computational domain large enough to make its boundary far away from the interface between magnetic fluid and non-magnetic fluid. In the microfluidic droplet control situations, the droplet is in close contact with the boundary (such as the tube wall).

To resolve this problem, a two-region method is used for ferrofluid free surface flow in magnetic field. As is illustrated by [Figure 3](#), region  $\Omega_1$ , named fluid region in this article, is occupied by phases of a ferrofluid and a non-magnetic one; region  $\Omega_2$ , named vacuum region here, is an extended region having a magnetic permeability of vacuum. In such computational domain, free surface flow is solved only in the fluid region, while the magnetic field is solved in fluid and vacuum regions. The boundaries of the vacuum region are designed far enough from the ferrofluid phase, such that the distortion effect on the magnetic field is negligible and reasonable boundary conditions can be applied for the magnetic potential. In this situation, whether the ferrofluid droplets exist or not, the external magnetic field in the computational domain is almost unchanged, so it is considered that the selected computational domain is sufficient for the

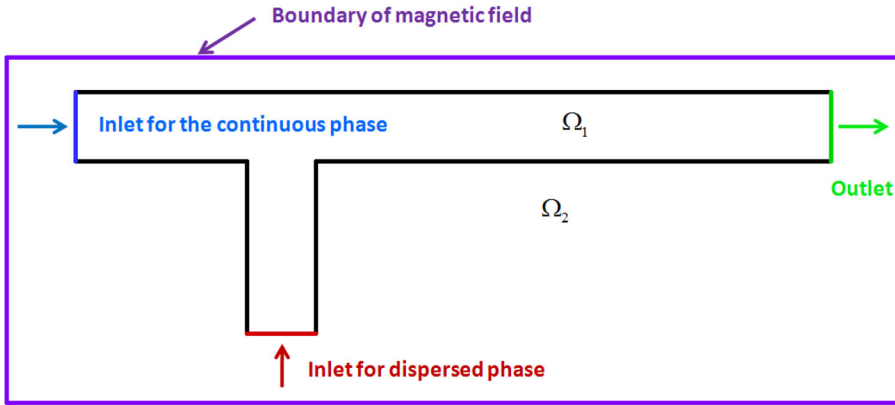


Figure 4. Two-region method for T-junction ferrofluid droplet generator.

problem. This two-region domain design is helpful for solving the problem in different regions, simplifying the solution process, therefore improving efficiency and accuracy.

### 3.3. Boundary conditions

As Figure 4 shows, the fluid flow is considered only in the fluid region in our computational domain, and correspondingly, its boundary conditions are specified on the border for the fluid region. Concretely, the ferrofluid phase flows in from the branch tube having an inlet velocity of 0.001 m/s, while the non-magnetic fluid flows in from the left of the main tube with a velocity of 0.01 m/s. Fully developed condition is set up at the outlet of the main tube. No-slip wall conditions were given on the other part of the border.

Since the fluid region is designed to be fully surrounded by the vacuum region, the boundary condition of the magnetic potential needs to be given only on the border of the vacuum region. For a specific cell face on boundary, the normal gradient of the magnetic scalar potential can be calculated based on the given magnetic field intensity:

$$\left(\frac{\partial\psi}{\partial n}\right)_b = \mathbf{n}_b \cdot (\nabla\psi)_b = -\mathbf{n}_b \cdot \mathbf{H}_b \quad (15)$$

where  $\mathbf{n}_b$  refers to the unit normal the cell face, and  $\mathbf{H}_b$  is the magnetic field strength calculated by Eq. (1). In this study, the magnetic potential value of the reference point (top left corner, its coordination is  $x = -0.0004$  m,  $y = 0.0016$  m) is set to 2.0 A. With this boundary condition the magnetic scalar potential can be uniquely determined.

### 3.4. Grid independent test

In this section, grid-independent examination is performed for the case without external magnetic field. Figure 5 shows the interface positions at 0.16 s of the ferrofluid droplet under the condition of pure two-phase flow without external magnetic field using four grid sizes. It can be seen that the phase interfaces obtained by using  $10\ \mu\text{m}$  and  $12.5\ \mu\text{m}$  are basically the same. In order to maintain a balance between accuracy and saving computing resources, all subsequent calculations in the present study adopt a grid resolution of  $10\ \mu\text{m}$ .

The adopted grid systems for the T-junction and the two-region are presented in Figure 6.

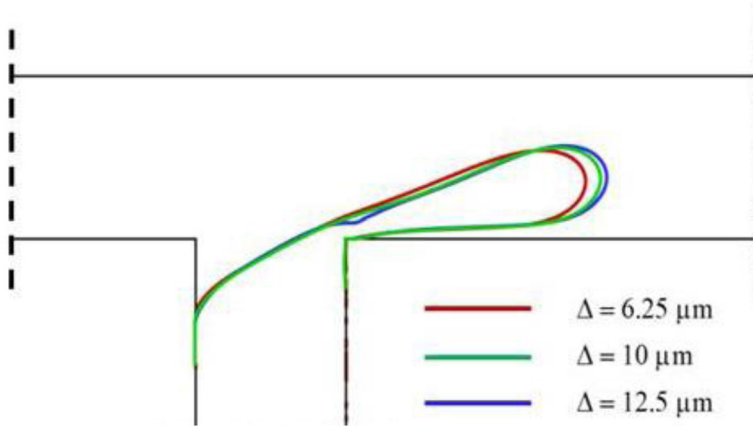
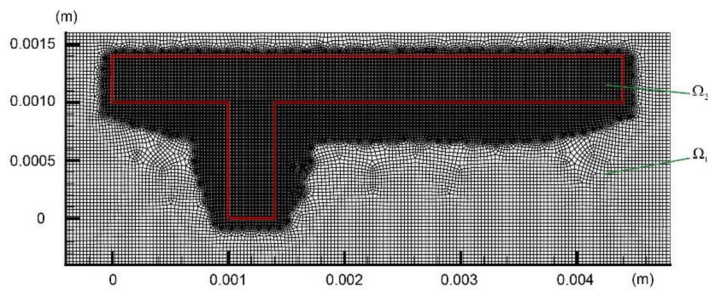
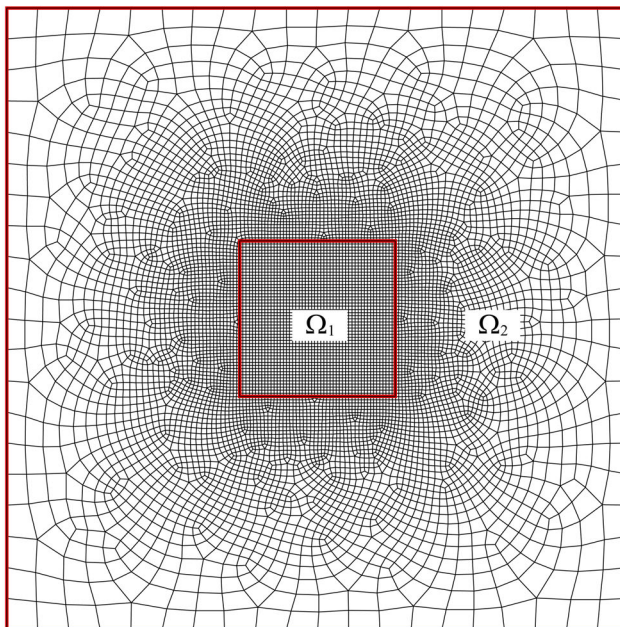


Figure 5. Results of grid independence test.



(a) Grid system of T-junction



(b) Grid system of two regions

Figure 6. Grid systems.

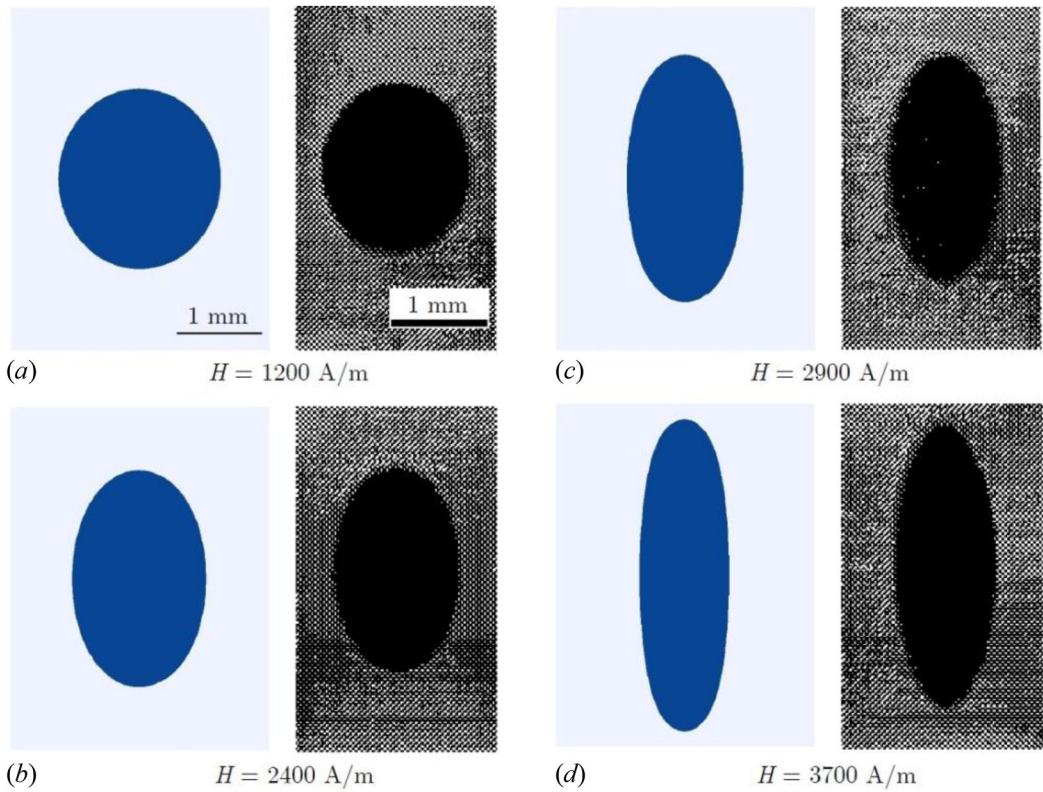


Figure 7. Ferrofluid droplet shapes at equilibrium.

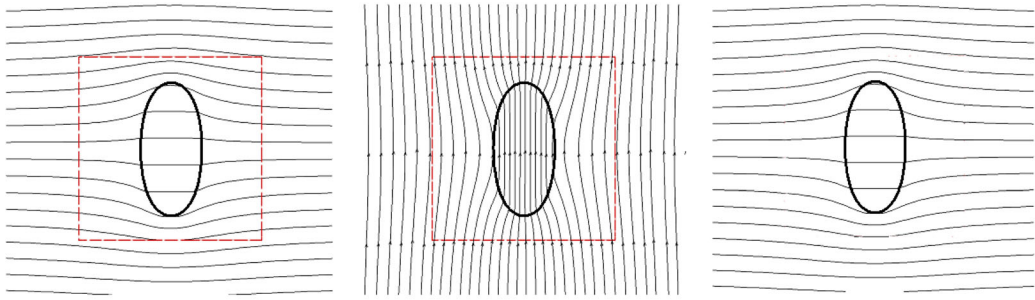
## 4. Results and discussion

In this section the process of droplet shape change under uniform magnetic field is investigated. First, a validation example is provided. Then the results of ferrofluid droplets formation process under non-uniform magnetic field are presented. Finally, the variation characteristics of droplets under different magnetic field forces are analyzed quantitatively.

### 4.1. Validation: droplet shape in a uniform magnetic field

To validate the numerical methods and the in-house code MHT used for the present study, we first performed a simulation on a single ferrofluid droplet deformation under a uniform magnetic field. As Figure 7 shows, a circular ferrofluid droplet having a radius  $R$  is placed at the center of an  $8R \times 8R$  domain. In the computation, we followed the parameters of the experiment reported by Flament et al. [32]. Concretely, the droplet radius  $R = 0.001$  m, the magnetic permeability of the ferrofluid  $\chi = 2.2$ , and the surface tension coefficient is  $0.00307$  N/m. The computational domain was discretized by  $100 \times 100$  uniform grid. Under the coupling effect of the magnetic field and the velocity field, the droplet will elongate along the direction of the magnetic field, and finally, a balance between the effects of the surface tension and the magnetic force will be reached.

Figure 7 shows the droplet shapes at equilibrium with applied uniform magnetic fields with  $H = 1200$  A/m,  $2400$  A/m,  $2900$  A/m and  $3700$  A/m, and the experimental results shown by the continuum pictures from Flament et al. [32] are included for comparison. It can be seen that the degree of deformation increases with the magnetic field intensity [16, 29]. Satisfied agreements



(a) Magnetic potential contours      (b) Magnetic field lines      (c) Result of one region

**Figure 8.** Numerical results of ferrofluid droplet deformation at  $H = 2900$  A/m.

are reached between numerical and experimental results except for the case with the largest magnetic field intensity ( $H = 3700$  A/m), where the droplet elongation was slightly over-predicted. In this regard, similar results were found by Afkhami et al. [13] in their numerical studies. As discussed by Afkhami et al. [13], the slightly over-predicted elongation lies in the constant surface tension coefficient used in the simulations which actually increases with the intensity of the applied magnetic field.

In order to assess the two-region method described in Section 3.2, we then performed the same problem using a two-region mesh displayed as Figure 6 (b). In this specific case, the magnetic field intensity was given as 2900 A/m. The fluid region ( $\Omega_1$ ) is a  $4R \times 4R$  square discretized by a  $50 \times 50$  uniform grid, and the vacuum region ( $\Omega_2$ ) is discretized by an unstructured mesh with greater grid size. The ferrofluid droplet shape at equilibrium along with the magnetic potential contours and magnetic field lines around it are plotted in Figure 8, where the red-dashed line refers to the interface between the two regions used in the computation. Compared with the droplet shape obtained by one-region approach (see Figure 8 (c)), one can see the same aspect ratio is achieved at equilibrium. Meanwhile, the magnetic field solved in the two regions shows a continuous feature across their boundary. The numerical results illustrated in this section confirm that the numerical methods and the developed code are reliable and can be applied for the present study.

#### 4.2. Droplet generation under external magnetic fields

Now attention is focused on the results of the problem described in Figure 1: the ferrofluid droplet generation in T-junction. The temporal evolution of the ferrofluid droplet at the T-junction without and with a magnetic field is shown in Figure 9, where the case without magnetic field is shown in the left, and the case with nonuniform magnetic field is in the right. In this figure, the zero time ( $t = 0$ s) is defined as the moment when the liquid level is flat and going to change.

From Figure 9, it can be seen that at first period ( $t = 0$ s to  $t = 0.18$ s) the formation process of ferrofluid is almost the same with or without magnetic field, those without magnetic field being only a little smaller. But afterwards, the ferrofluid droplets grow quite differently for the two cases. It can be seen from the right column of Figure 9, the formation process of ferrofluid droplets in magnetic field can be divided into three stages: the expansion, extrusion and pinch-off. In the expansion stage, from time  $t = 0$ s to  $t = 0.2$ s, the flow of two phases gradually fills the T-junction in the side pipe (Branch 1). Because the magnetic field force is opposite to the flow direction of the ferrofluid, less ferrofluid flows into the downstream channel under the obstruction of both the magnetic force and the continuous phase. At this stage, the tip of the ferrofluid droplet gradually expands radially and laterally in the main channel, and the droplet gradually plumps

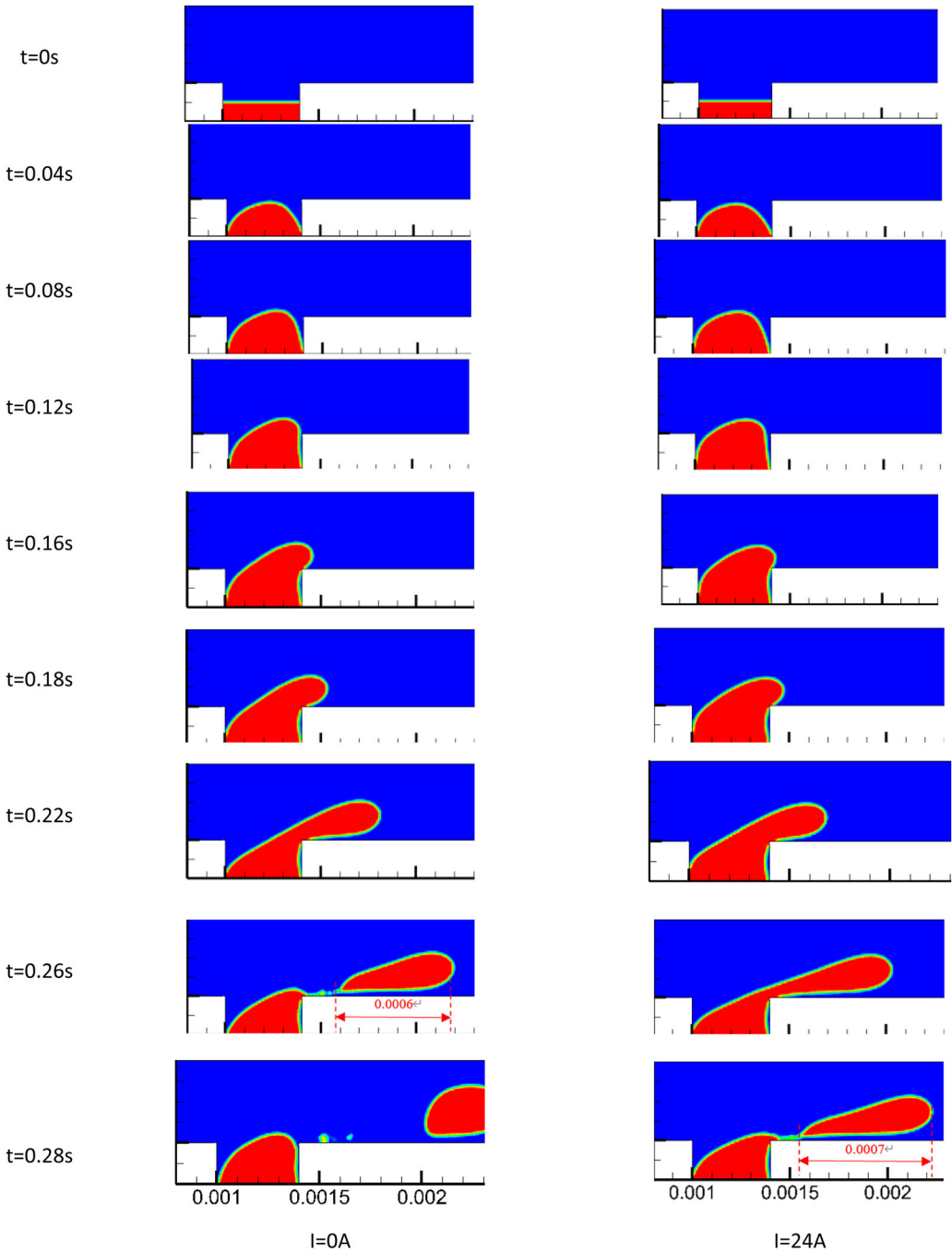


**Figure 9.** Evolution of the ferrofluid droplet formation process. Left column: no magnetic field; right column: nonuniform magnetic field.

up to the radial maximum ( $t = 0.22$  s), which is the end of this stage. Subsequently, the ferrofluid droplet forming process enters the extrusion stage ( $t = 0.22$  s  $\sim$   $t = 0.26$  s). At this stage, the extrusion pressure and shear force of the droplet play a leading role in driving the droplet tip to move downstream. The outline of the dispersed neck gradually changes from convex to concave and becomes thinner. After entering the pinch-off stage ( $t = 0.26$  s  $\sim$   $t = 0.28$  s), the dispersed neck

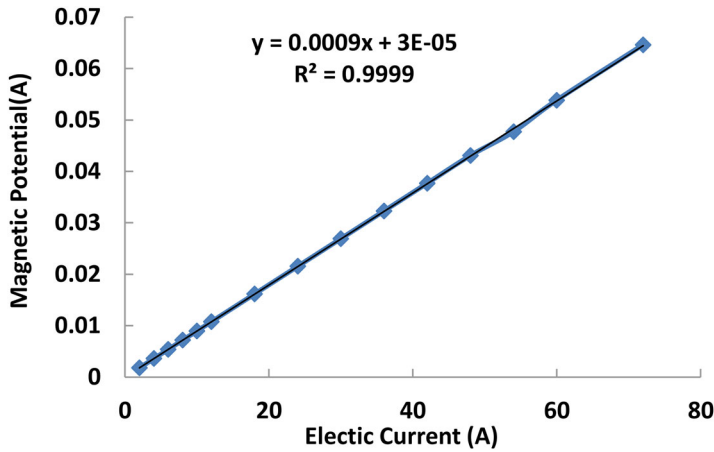


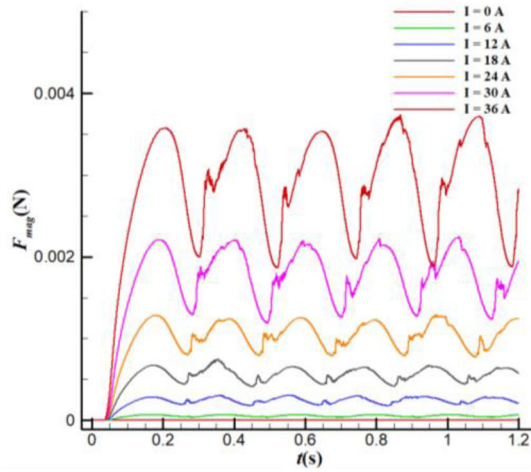
**Figure 10.** Relationship of magnetic potential and current intensity at position (0.0014 m, 0.0012 m).

thins rapidly near the T-junction. At time  $t = 0.28$  s, the extrusion pressure and shear force finally overcome the resistance of both magnetic force and interfacial tension, so the dispersed neck fracture occurs, and then a new ferrofluid droplet is formed. The magnetic field generated by the wires on the side of the microfluidic T-junction attracts the ferrofluid and impedes the flow of the dispersed phase, making it more difficult for the continuous phase to pinch off the dispersed phase to form new droplets. The pinch off time and dispersed thread length of the ferrofluid droplet formation with and without magnetic fields are different. In the case without magnetic field, the dispersed neck is broken at  $t = 0.26$  s and the length of the dispersed thread is 0.0006 m. Whereas, the case with a magnetic field, the dispersed neck breaks until  $t = 0.28$  s and the length of the dispersed thread is 0.0007 m. Obviously, the magnetic field designed in this article hinders the formation of droplets, prolongs the formation cycle of ferrofluid droplets, reduces its formation frequency, increases the radius of curvature of the neck of droplets, and thus increases the size of the droplet in the radial direction of the main channel.

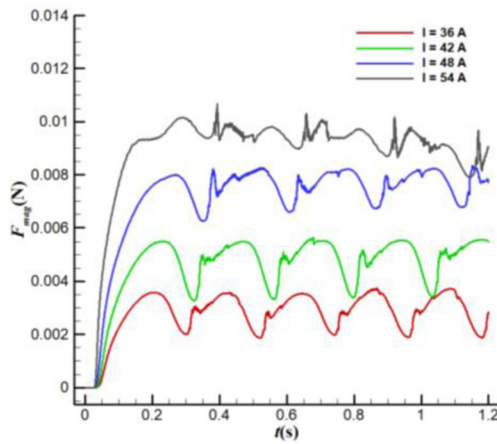
#### 4.3. Influences of the magnetic field intensity

In this subsection, the influence of the nonuniform magnetic field intensity on the deformation of ferrofluid droplet is analyzed in detail. As mentioned above, the magnetic field intensity is controlled by the electric current values. For example, the relationship of magnetic potential and current intensity at position (0.0014 m, 0.0012 m) is presented in Figure 10. It can be found that the magnetic potential value is directly proportional to the electric current value, and their relationship can be approximated with a function  $y = 0.0009x + 3 \times 10^{-5}$ . Therefore, the effect of the magnetic field intensity can be replaced by the influence of the electric current intensity on the droplet deformation.

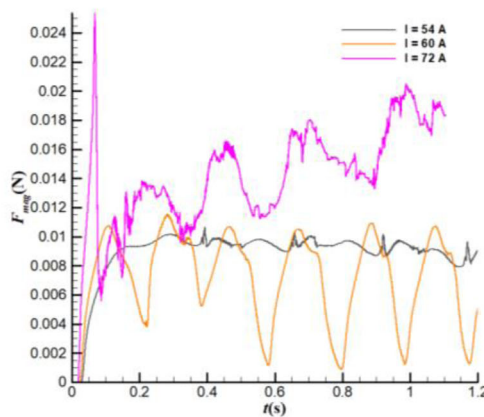
The variation of magnetic force on a single ferrofluid droplet with electric current intensity from 0 A to 72 A is further calculated to explore their relationship under the generation process of ferrofluid droplets and the results are presented in Figure 11. As the current intensity increases, the magnetic force of the ferrofluid droplet increases and decreases periodically, especially for electric current intensity is less than 60 A. It is to be noted that the minimum magnetic force for  $I = 60$  A is smaller than that for  $I = 54$  A, and the magnetic force for  $I = 72$  A fluctuates periodically and continues to increase. To illustrate this abnormal phenomenon, locations and sizes of ferrofluid droplet for  $I = 54$  A, 60 A, and 72 A at several times are exhibited in Figure 12. When the electric current intensity increases to  $I = 60$  A, the departure characteristics begins to



(a) From 0 to 36 A



(b) From 36A to 54A



(c) From 54 A to 72A

**Figure 11.** Different magnetic force imposing on the droplet.

change. Specifically, for  $I = 60$  A, some ferrofluid will be adsorbed close to the upper wall of the main channel, which leads to a droplet with smaller departure diameter, so its corresponding magnetic force is smaller. Whereas, when the current intensity continues to increase to  $I = 72$  A,

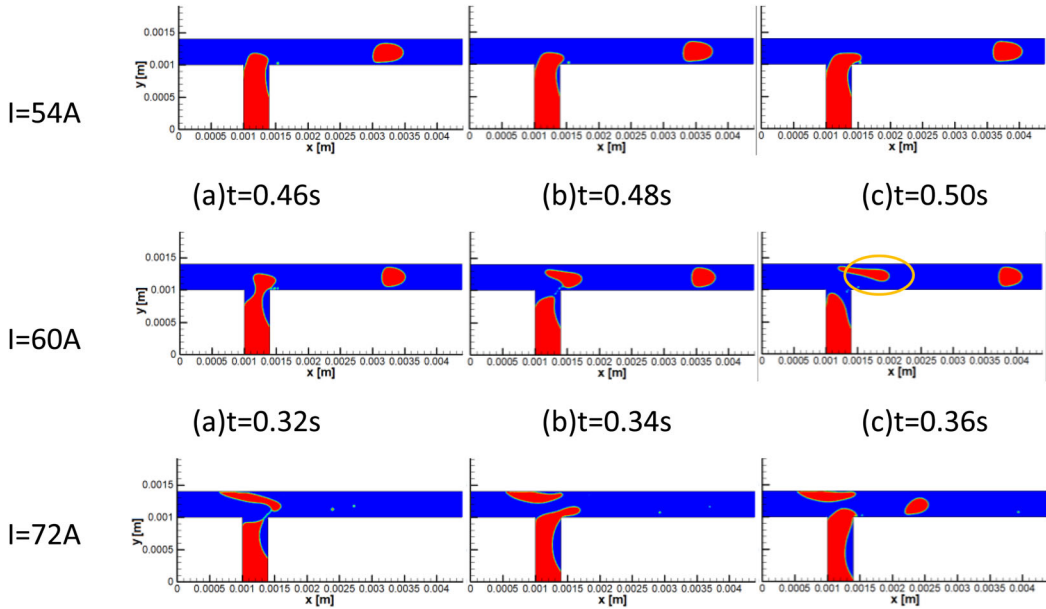


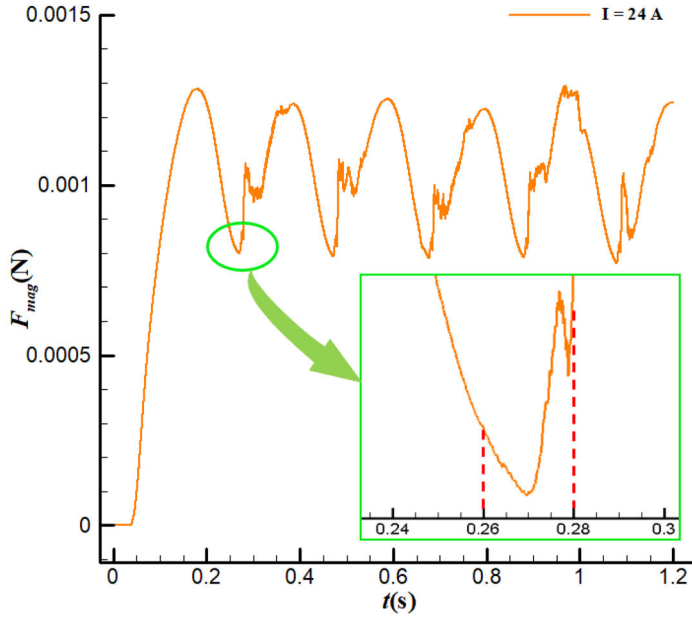
**Figure 12.** Locations of droplet for  $I = 54\text{A}$ ,  $60\text{A}$ , and  $72\text{A}$  at several different times.

the ferrofluid is adsorbed on the top of the main channel, so the magnetic force progressively increases with the expansion of the adsorption area.

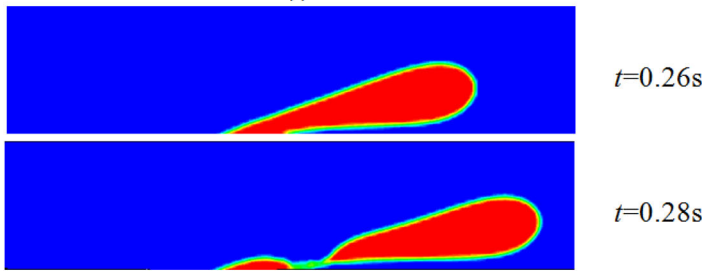
It can be found from [Figure 11](#), in the cases with the current intensity less than  $54\text{A}$  ([Figure 11 \(a\) and \(b\)](#)), the magnetic force on the ferrofluid droplet presents a significant periodic variation. Taking the case with current intensity  $I = 24\text{A}$  (see [Figure 13](#)) as an example, the magnetic force on the droplet gradually increases to its maximum when the dispersed neck expands, afterwards decreases to its minimum which is due to the tail of dispersed neck is thinned until fracture under the damping effect of continuous phase. When  $t = 0.27\text{s}$ , the dispersed neck ruptures, the corresponding magnetic force reaches the minimum and its value is  $0.0007\text{N}$ , and at this moment a whole generation cycle is completed. Subsequently, a new ferrofluid droplet generates and grows gradually, and the magnetic force will repeat the above process.

To quantify the departure period of ferrofluid droplet with different electric current intensities which are less than  $60\text{A}$ , the departure frequency of ferrofluid droplet under different electric current values is calculated and plotted in [Figure 14](#). As can be seen, with the increase of current intensity, the departure frequency of the ferrofluid droplet decreases, that is the departure period increases. The evolution of departure frequency can be divided into three stage: fluctuation stage, decline stage, and upsurge stage.

In the fluctuation stage ( $2\text{A} \sim 12\text{A}$ ), the existence of magnetic field has little effect on the formation of ferrofluid droplets, and the departure frequency is basically maintained at about  $5.15\text{Hz}$ . While in the decline stage ( $12\text{A} \sim 54\text{A}$ ), the departure frequency decreases monotonically along with the increase of the current intensity. The departure frequency falls nearly in a quadratic form with current intensity. The quadratic function is determined by the least square method as shown in [Figure 14 \(b\)](#). In this stage, although the magnetic force can promote the droplet retention with the increasing the current intensity, it is not enough to adsorb the ferrofluid droplet to the upper wall of main channel. Therefore, the departure period is prolonged by the increasing current intensity. The magnetic force can be increased enough to adsorb the ferrofluid droplet to the radial upper wall of the main channel, when continue to increase of the current intensity ( $54\text{A} \sim 60\text{A}$ ). The departure characteristic at this stage is different with that in the decline stage, which is consistent with the characteristics shown in [Figure 11](#).



(a) Force vs time



(b) Droplet neck rupture process

Figure 13. The magnetic force imposed on the droplet during the departure process.

To further illustrate the effect of magnetic force on the ferrofluid, the departure diameter of the ferrofluid droplet is used. In this article the image processing method is used to calculate the departure diameter and the resulted image is shown in Figure 15. As shown in the figure, the red component of Figure 15 (a) is supposed to the ferrofluid, the blue component is the continuous phase, and the green part is the interface of the two phases. The outer boundary of the red part is used to distinguish the ferrofluid droplet and the continuous phase. The final processing result is shown in Figure 15 (b). Based on the images the equivalent departure diameter of the ferrofluid droplet can be calculated by:

$$d_{departure} = 2.0 \left( \frac{A_{drop}}{\pi} \right)^{0.5} \Delta x_{pixel} \quad (16)$$

where  $A_{drop}$  represents the number of image pixels occupied by ferrofluid droplet,  $\Delta x_{pixel}$  is the physical size of single pixel.

The departure diameter is investigated by varying the electric current intensity from 0 A to 60 A while keeping other parameters unchanged. According to the results of the image processing

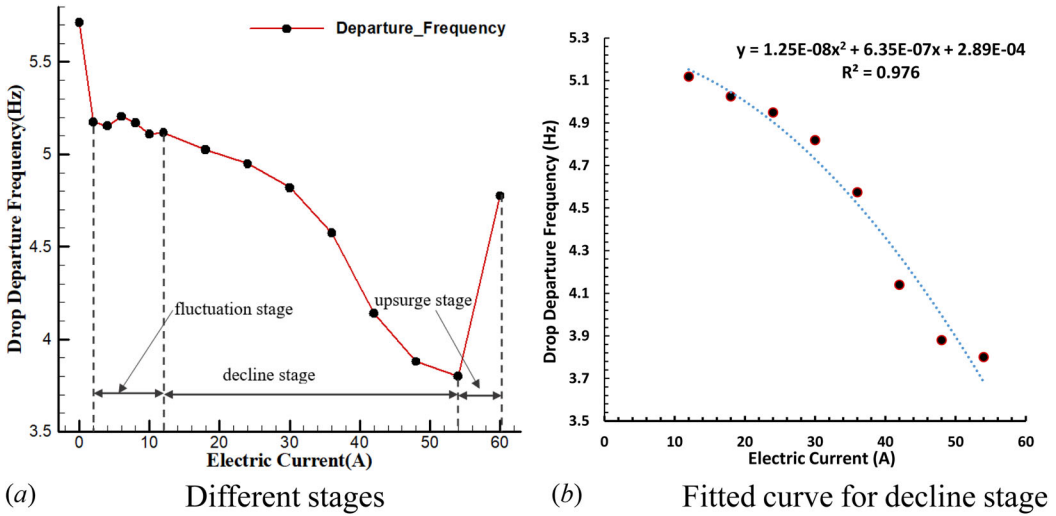


Figure 14. The departure frequency of ferrofluid droplet under different electric current intensities.

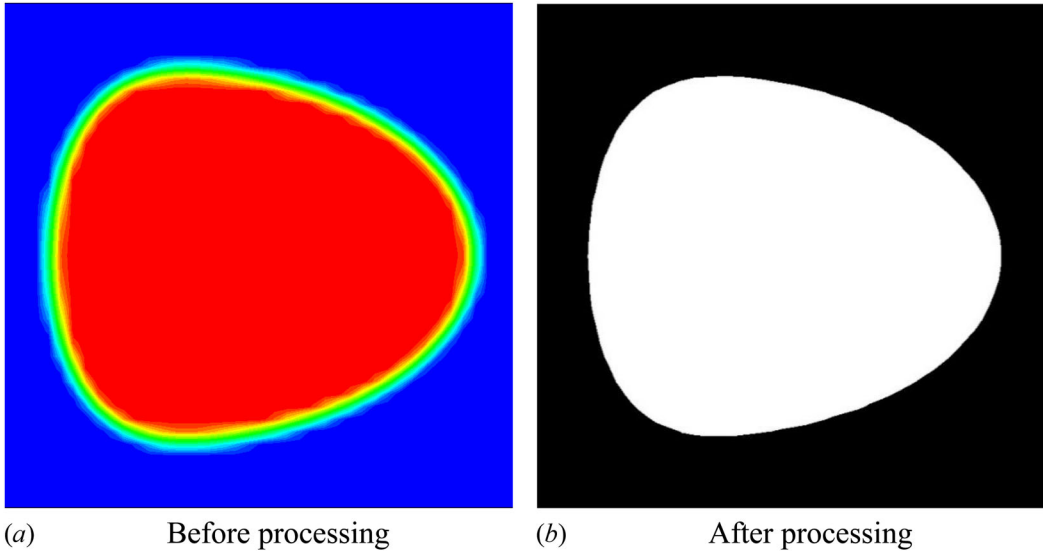


Figure 15. The image for departure diameter calculation.

method, the departure diameter of a ferrofluid droplet under the above conditions are obtained as shown in Figure 16. It is obvious that the magnetic force does affect the formation of ferrofluid droplet.

This result is consistent with the characteristics shown in Figure 14. The variation of departure diameter under different electric current intensities also can be segmented into three stages: fluctuation stage, upswing stage, and slump stage. In the fluctuation stage ( $I = 0 \sim 12$  A), the departure diameter of ferrofluid droplet is fluctuated around 0.00031 m. When the electric current intensity continues to increase, it enters the upswing stage, and the departure diameter rises rapidly in a quadratic form with current intensity. The expression of the quadratic function is determined by the least square method as shown in Figure 16 (b). When the current intensity exceeds 54 A, the departure diameter drops sharply, that is, drop diameter variation enters into the slump stage.

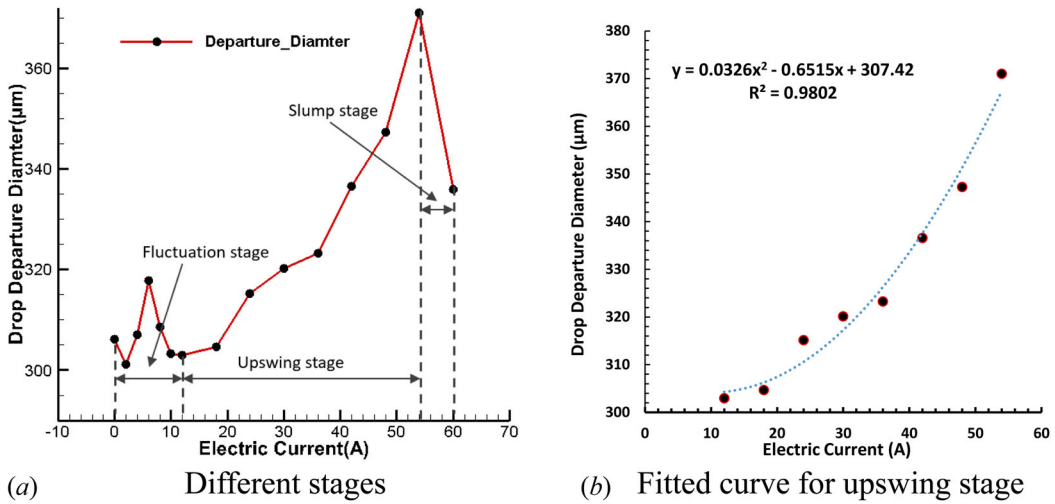


Figure 16. Departure diameter of the ferrofluid droplet under different magnetic field intensity.

## 5. Conclusions

In this study, the generation characteristics of ferrofluid droplets in a microfluidic T-junction under the influence of nonuniform magnetic field has been studied numerically. Specifically, a coupled volume-of-fluid and level-set interface tracking method (VOSET) was applied for handling the moving boundary. A two-region method is designed for ferrofluid free surface flow in magnetic field. The numerical methods were implemented by an in-house CFD code, named as MHT, designed for solving multi-region heat transfer and fluid flow. Based on this, formation of ferrofluid droplets under various magnetic field strength are studied in detail. The main conclusions of this study are:

1. The magnetic field strength can be effectively controlled by two electrified straight wires instead of permanent magnet. In this condition, the produced magnetic force can control ferrofluid droplet formation.
2. As the current intensity increases, the magnetic force of the ferrofluid droplet increases and decreases periodically, especially for electric current intensity is less than 60A.
3. The evolution of departure frequency (departure diameter) with the increase of electric current intensity can be divided into three stages: fluctuation stage, decline (upswing) stage, and upsurge (slump) stage.
4. The size and period of ferrofluid droplet formation can be effectively controlled when  $I$  is within the range of [12A, 54A]. In these cases, increasing current intensity can prolong the ferrofluid droplet generation period.
5. When the current intensity exceeds 60A, the ferrofluid will be absorbed on the upper wall of the main channel.

All findings obtained this article will provide valuable references for accurately controlling the size and frequency of ferrofluid droplets, thus promoting the further development of its applications in many fields including biologic analyses, micropumps, and drug delivery.

## Conflict of interest

The authors declared that there is no conflict of interest.

## Funding

This work is supported by the China Postdoctoral Science Foundation (2018M6333506) and the Foundation for Innovative Research Groups of the National Natural Science Foundation of China (No. 51721004).

## References

- [1] K. Raj and R. Moskowitz, "Commercial applications of ferrofluids," *J. Magnetism Magnetic Materials*, vol. 85, no. 1-3, pp. 233–245, 1990. DOI: [10.1016/0304-8853\(90\)90058-X](https://doi.org/10.1016/0304-8853(90)90058-X).
- [2] S. A. Majetich, T. Wen and R. A. Booth, "Functional magnetic nanoparticle assemblies: Formation, collective behavior, and future directions," *ACS Nano*, vol. 5, no. 8, pp. 6081–6084, 2011. DOI: [10.1021/nn202883f](https://doi.org/10.1021/nn202883f).
- [3] Z. M. Wang, R. G. Wu, Z. P. Wang and R. V. Ramanujan, "Magnetic trapping of bacteria at low magnetic fields," *Sci Rep*, vol. 6, no., pp. 269452016. DOI: [10.1038/srep26945](https://doi.org/10.1038/srep26945).
- [4] Y. J. Chang, C. Y. Hu and C. H. Lin, "A microchannel immunoassay chip with ferrofluid actuation to enhance the biochemical reaction," *Sensors Actuators B Chemical*, vol. 182, pp. 584–591, 2013. DOI: [10.1016/j.snb.2013.03.078](https://doi.org/10.1016/j.snb.2013.03.078).
- [5] K. Hayashi, W. Sakamoto and T. Yogo, "Drug delivery: Smart ferrofluid with quick gel transformation in tumors for mri-guided local magnetic thermochemotherapy," *Adv. Funct. Mater.*, vol. 26, no. 11, pp. 1852–1852, 2016. DOI: [10.1002/adfm.201670071](https://doi.org/10.1002/adfm.201670071).
- [6] J. Zeng, Y. Deng, P. Vedantam, T.-R. Tzeng and X. Xuan, "Magnetic separation of particles and cells in ferrofluid flow through a straight microchannel using two offset magnets," *J. Magnetism Magnetic Materials*, vol. 346, pp. 118–123, 2013.
- [7] M. Fabian, P. Burda, M. Viková and R. Huňady, "The Influence of magnetic field on the separation of droplets from ferrofluid jet," *J. Magnetism Magnetic Materials*, vol. 431, no. 6, pp. 196–200, 2017. DOI: [10.1016/j.jmmm.2016.09.052](https://doi.org/10.1016/j.jmmm.2016.09.052).
- [8] Q. Zhang, H. Li, C. Zhu, T. Fu, Y. Ma and H. Z. Li, "Micro-magnetofluidics of ferrofluid droplet formation in a T-junction," *Colloids Surfaces A Physicochemical Engineering Aspects*, vol. 537, pp. 572–579, 2018. DOI: [10.1016/j.colsurfa.2017.10.056](https://doi.org/10.1016/j.colsurfa.2017.10.056).
- [9] X. Sun, C. Zhu, T. Fu, Y. Ma and H. Z. Li, "Dynamics of droplet breakup and formation of satellite droplets in a microfluidic T-junction," *Chemical Engineering sci.*, vol. 188, pp. 158–169, 2018. DOI: [10.1016/j.ces.2018.05.027](https://doi.org/10.1016/j.ces.2018.05.027).
- [10] A. Favakeh, M. A. Bijarchi and M. B. Shafii, "Ferrofluid droplet formation from a nozzle using alternating magnetic field with different magnetic coil positions," *J. Magnetism Magnetic Materials*, vol. 498, pp. 166134, 2020.
- [11] O. Lavrova, G. Matthies, V. Polevikov and L. Tobiska, "Numerical modeling of the equilibrium shapes of a ferrofluid drop in an external magnetic field," *Proc. Appl. Math. Mech.*, vol. 4, no. 1, pp. 704–705, 2004. DOI: [10.1002/pamm.200410333](https://doi.org/10.1002/pamm.200410333).
- [12] M. S. Korlie, A. Mukherjee, B. G. Nita, J. G. Stevens, A. D. Trubatch and P. Yecko, "Modeling bubbles and droplets in magnetic fluids," *J. Physics: Condensed Matter*, vol. 20, no. 20, pp. 204143, 2008.
- [13] S. Afkhami, et al., "Deformation of a hydrophobic ferrofluid droplet suspended in a viscous medium under uniform magnetic fields," *J. Fluid Mech.*, vol. 663, pp. 358–384, 2010. DOI: [10.1017/S0022112010003551](https://doi.org/10.1017/S0022112010003551).
- [14] H. Ki, "Level set method for two-phase incompressible flows under magnetic fields," *Computer Physics commun.*, vol. 181, no. 6, pp. 999–1007, 2010. DOI: [10.1016/j.cpc.2010.02.002](https://doi.org/10.1016/j.cpc.2010.02.002).
- [15] J. Liu, S. H. Tan, Y. F. Yap, Y. N. Min and N. T. Nguyen, "Numerical and experimental investigations of the formation process of ferrofluid droplets," *Microfluid Nanofluid.*, vol. 11, no. 2, pp. 177–187, 2011. DOI: [10.1007/s10404-011-0784-7](https://doi.org/10.1007/s10404-011-0784-7).
- [16] J. Liu, Y. F. Yap and N. T. Nguyen, "Numerical study of the formation process of ferrofluid droplets," *Physics Fluids*, vol. 23, no. 7, pp. 072008–072422, 2011. DOI: [10.1063/1.3614569](https://doi.org/10.1063/1.3614569).
- [17] D. Shi, Q. Bi and R. Zhou, "Numerical simulation of a falling ferrofluid droplet in a uniform magnetic field by the VOSET method," *Numerical Heat Transfer Applicat.*, vol. 66, no. 2, pp. 144–164, 2014. DOI: [10.1080/10407782.2013.869459](https://doi.org/10.1080/10407782.2013.869459).
- [18] D. L. Sun and W. Q. Tao, "A coupled volume-of-fluid and level set (VOSET) method for computing incompressible two-phase flows," *Int. J. Heat Mass Transfer*, vol. 53, no. 4, pp. 645–655, 2010. DOI: [10.1016/j.ijheatmasstransfer.2009.10.030](https://doi.org/10.1016/j.ijheatmasstransfer.2009.10.030).
- [19] A. Ghaffari, S. H. Hashemabadi and M. Bazmi, "CFD simulation of equilibrium shape and coalescence of ferrofluid droplets subjected to uniform magnetic field," *Colloids Surfaces A Physicochemical Engineering Aspects*, vol. 481, pp. 186–198, 2015. DOI: [10.1016/j.colsurfa.2015.04.038](https://doi.org/10.1016/j.colsurfa.2015.04.038).

- [20] M. Sussman and E. G. Puckett, "A coupled level set and volume-of-fluid method for computing 3D and axisymmetric incompressible Two-Phase Flows," *J. Computational Physics*, vol. 162, no. 2, pp. 301–337, 2000. DOI: [10.1006/jcph.2000.6537](https://doi.org/10.1006/jcph.2000.6537).
- [21] U. Sen, S. Chatterjee, S. Sen, M. K. Tiwari, A. Mukhopadhyay and R. Ganguly, "Dynamics of magnetic modulation of ferrofluid droplets for digital microfluidic applications," *J. Magnetism Magnetic Materials*, vol. 421, no. 1, pp. 165–176, 2017. DOI: [10.1016/j.jmmm.2016.07.048](https://doi.org/10.1016/j.jmmm.2016.07.048).
- [22] M. Habera and J. Hron, "Modelling of a free-surface ferrofluid flow," *J. Magnetism Magnetic Materials*, vol. 431, no. 6, pp. 157–160, 2017. DOI: [10.1016/j.jmmm.2016.10.045](https://doi.org/10.1016/j.jmmm.2016.10.045).
- [23] V. B. Varma, et al., "Control of ferrofluid droplets in microchannels by uniform magnetic fields," *IEEE Magn. Lett*, vol. 7, pp. 1–5, 2016. Art no. 2105305. DOI: [10.1109/LMAG.2016.2594165](https://doi.org/10.1109/LMAG.2016.2594165).
- [24] A. Ray, et al., "Magnetic droplet merging by hybrid magnetic fields," *IEEE Magn. Lett*, vol. 7, pp. 1–5, 2016. Art no. 6507705. DOI: [10.1109/LMAG.2016.2613065](https://doi.org/10.1109/LMAG.2016.2613065).
- [25] M. Aboutalebi, M. A. Bijarchi, M. B. Shafii and S. K. Hannani, "Numerical investigation on splitting of ferrofluid microdroplets in T-junctions using an asymmetric magnetic field with proposed correlation," *J. Magnetism Magnetic Materials*, vol. 447, no. 2, pp. 139–149, 2018. DOI: [10.1016/j.jmmm.2017.09.053](https://doi.org/10.1016/j.jmmm.2017.09.053).
- [26] R. M. Hassan, Z. Jie and W. Cheng, "Deformation of a ferrofluid droplet in simple shear flows under uniform magnetic fields," *Physics Fluids*, vol. 30, no. 9, pp. 092002, 2018. DOI: [10.1063/1.5047223](https://doi.org/10.1063/1.5047223).
- [27] A. Ghaderi, M. H. Kayhani and M. Nazari, "Numerical investigation on falling ferrofluid droplet under uniform magnetic field," *European J. Mechanics-B/Fluids*, vol. 72, pp. 1–11, 2018. DOI: [10.1016/j.euromechflu.2018.04.008](https://doi.org/10.1016/j.euromechflu.2018.04.008).
- [28] C. Paolo, L. Marcello and M. S. N. Oliveira, "Deformation of a ferrofluid droplet in a simple shear flow under the effect of a constant magnetic field," *Computers Fluids*, vol. 173, pp. 313–323, 2018. DOI: [10.1016/j.compfluid.2018.06.024](https://doi.org/10.1016/j.compfluid.2018.06.024).
- [29] K. Ling, K.-K. Guo, S. Zhang and W.-Q. Tao, "A numerical investigation on dynamics of ferrofluid droplet in nonuniform magnetic field," *Numerical Heat Transfer, Part A: Applicat.*, vol. 75, no. 10, pp. 690–707, 2019. DOI: [10.1080/10407782.2019.1609277](https://doi.org/10.1080/10407782.2019.1609277).
- [30] K. S. Lok, Y. C. Kwok, P. P. F. Lee and N. T. Nguyen, "Ferrofluid plug as valve and actuator for whole-cell PCR on chip," *Sensors Actuators B*, vol. 166–167, pp. 893–897, 2012. DOI: [10.1016/j.snb.2012.03.001](https://doi.org/10.1016/j.snb.2012.03.001).
- [31] D. L. Youngs, "Time-dependent multi-material flow with large fluid distortion," *Numerical Methods for Fluid Dynamics*, New York: Academic, 1985, pp. 273–285.
- [32] C. Flament, S. Lacia, J. C. Bacri, A. Cebers, S. Neveu and R. Perzynski, "Measurements of ferrofluid surface tension in confined geometry," *Phys Rev E Stat Phys Plasmas Fluids Relat Interdiscip Topics*, vol. 53, no. 5, pp. 4801–4806, 1996. DOI: [10.1103/physreve.53.4801](https://doi.org/10.1103/physreve.53.4801).